BEST AVAILABLE IMAGES

Defective images within this document are accurate representations of the original documents submitted by the applicant.

Defects in the images may include (but are not limited to):

- BLACK BORDERS
- TEXT CUT OFF AT TOP, BOTTOM OR SIDES
- FADED TEXT
- ILLEGIBLE TEXT
- SKEWED/SLANTED IMAGES
- COLORED PHOTOS
- BLACK OR VERY BLACK AND WHITE DARK PHOTOS
- GRAY SCALE DOCUMENTS

IMAGES ARE BEST AVAILABLE COPY.

As rescanning documents *will not* correct images, please do not report the images to the Image Problem Mailbox.

EXHIBIT 1

THE JOURNAL OF BIOLOGICAL CHEMISTRY Vol. 272, No. 20, Issue of May 16, pp. 13094–13102, 1997
Printed in U.S.A.

Function of Disintegrin-like/Cysteine-rich Domains of Atrolysin A

INHIBITION OF PLATELET AGGREGATION BY RECOMBINANT PROTEIN AND PEPTIDE ANTAGONISTS*

(Received for publication, August 19, 1996, and in revised form, March 11, 1997)

Li-Guo Jia, Xiao-Ming Wang, John D. Shannon, Jon B. Bjarnason‡, and Jay W. Fox§

From the Department of Microbiology, University of Virginia Health Sciences Center, Charlottesville, Virginia 22908 and ‡Science Institute, University of Iceland, Reykjavik, Iceland

Snake venom hemorrhagic metalloproteinase toxins that have metalloproteinase, disintegrin-like and cysteine-rich domains are significantly more potent than toxins with only a metalloproteinase domain. The disintegrin-like domains of these toxins differ from the disintegrin peptides found in crotalid and viperid venoms by the nature of their different disulfide bond structure and, in lieu of the disintegrins' signature Arg-Gly-Asp (RGD) integrin binding sequence, there is an *XXCD* disulfide-bonded cysteinyl sequence in that region. Due to these apparent differences, the contribution to the overall function of the hemorrhagic metalloproteinases by the disintegrin-like domain has been unknown. In this investigation we have expressed in insect cells the disintegrin-like/cysteine-rich (DC) domains of the *Crotalus atrox* hemorrhagic metalloproteinase atrolysin A and demonstrated that the recombinant protein (A/DC) can inhibit collagen- and ADP-stimulated platelet aggregation. Using synthetic peptides, we have evidence that the region of the disintegrin-like domain that is positionally analogous to the RGD loop of the disintegrins is the site responsible for inhibition of platelet aggregation. For these synthetic peptides to have significant inhibitory activity, the -RSECD- cysteinyl residue must be constrained by participation in a disulfide bond with another cysteinyl residue. The two acidic amino acids adjacent to the middle cysteinyl residue in these peptides are also important for biological activity. These studies emphasize a functional role for the disintegrin-like domain in toxins and suggest structural possibilities for the design of antagonists of platelet aggregation.

The distinctive characteristic of envenomation by a crotalid or viperid snake is local and in severe cases systemic hemorrhage. The profuse hemorrhage observed is usually due to the synergistic action of a large number of toxins in the venom (1, 2). However, the toxins primarily responsible for hemorrhage are snake venom zinc metalloproteinases (SVMPs),[1] which are members of the reprolysin subfamily of the M12 family of metalloproteinases (3–5). These toxins, as isolated from crude venom, belong to one of three related structural classes, P-I, -II, and -III, which primarily differ from one another by the presence of additional domains on the carboxyl side of the metalloproteinase domain (4). The P-I class has only a metalloproteinase domain, whereas the P-II class has a disintegrin or disintegrin-like domain carboxyl to the proteinase domain. The P-III class metalloproteinases have yet another domain, the cysteine-rich domain, which is found carboxyl to the disintegrin-like domain.

The P-III class of venom metalloproteinases is related to the ADAMs/MDCs group of type I integral membrane protein. These protein groups have homologous proteinase, disintegrin-like and cysteine-rich domain structures, and these proteinases are classified as members of the reprolysin subfamily of metalloproteinases (5). However, the ADAMs/MDC proteinases possess additional carboxyl-terminal structures comprised of epidermal growth factor-like, transmembrane, and cytoplasmic domains (6–9).

The biological function of many of the ADAMs/MDCs proteins is unclear, except for the fertilins α and β, which are involved in egg-sperm fusion (10), meltrins, which are involved in myoblast fusion (11), and KUZ, a *Drosophila* protein which participates in neurogenesis (12). In the case of the fertilins, which are the most functionally characterized of the group, the disintegrin-like domain of fertilin is thought to modulate egg-sperm fusion by interaction of the disintegrin-like domain of the sperm fertilin with the $\alpha_6\beta_1$ integrin on the egg (13). The structural features of the disintegrin-like domain important in this interaction are not known with certainty but may involve a specific sequence of the disintegrin-like domain of fertilin (13).

Disintegrins are peptides, isolated from the venoms of crotalid and viperid snakes, and range in length from 49 to 84 amino acid residues. They function as potent inhibitors of platelet aggregation (14–16). The RGD sequence in a 13-residue β-loop structure (the RGD loop) is the critical structural moiety responsible for biological activity and is central to the interaction of the disintegrins with the platelet integrin $\alpha_{IIb}\beta_3$ (17, 18). The disulfide bond structure of these peptides also contributes to the activity of the disintegrins (19, 20). The disintegrins are derived from homologous precursors of the P-II class of snake venom metalloproteinases by the processing of precursors comprised of pre-, pro-, metalloproteinase, and disintegrin domains (21).

The homologous region of the class P-III SVMPs differs from the disintegrins and their P-II precursors in several ways. Due to these differences, we have termed them "disintegrin-like" domains. Disintegrin-like domains have two additional cysteinyl residues compared with the disintegrins, and therefore the disulfide bond arrangement is likely to be different. We hypothesize that one of these cysteines is involved in a disulfide bond

* This work was supported by National Institutes of Health Grant GM49042 (to J. W. F.). The costs of publication of this article were defrayed in part by the payment of page charges. This article must therefore be hereby marked "*advertisement*" in accordance with 18 U.S.C. Section 1734 solely to indicate this fact.

§ To whom correspondence should be addressed: Dept. of Microbiology, Box 441 Jordan Hall, UVA Health Sciences Center, Charlottesville, VA 22908. Tel.: 804-924-0050; Fax: 804-982-2514.

[1] The abbreviations used are: SVMPs, snake venom metalloproteinases; Acm, acetoamidomethyl; AcNMPV: *A. californica* nuclear polyhedrosis virus; ADAMs, a disintegrin-like and metalloproteinase proteins; A/DC, recombinant disintegrin-like/cysteine-rich protein from atrolysin A; MALD-TOF, matrix assisted laser desorption-time of flight; MDCs, metalloproteinase disintegrin-like cysteine-rich proteins; PAGE, polyacrylamide gel electrophoresis.

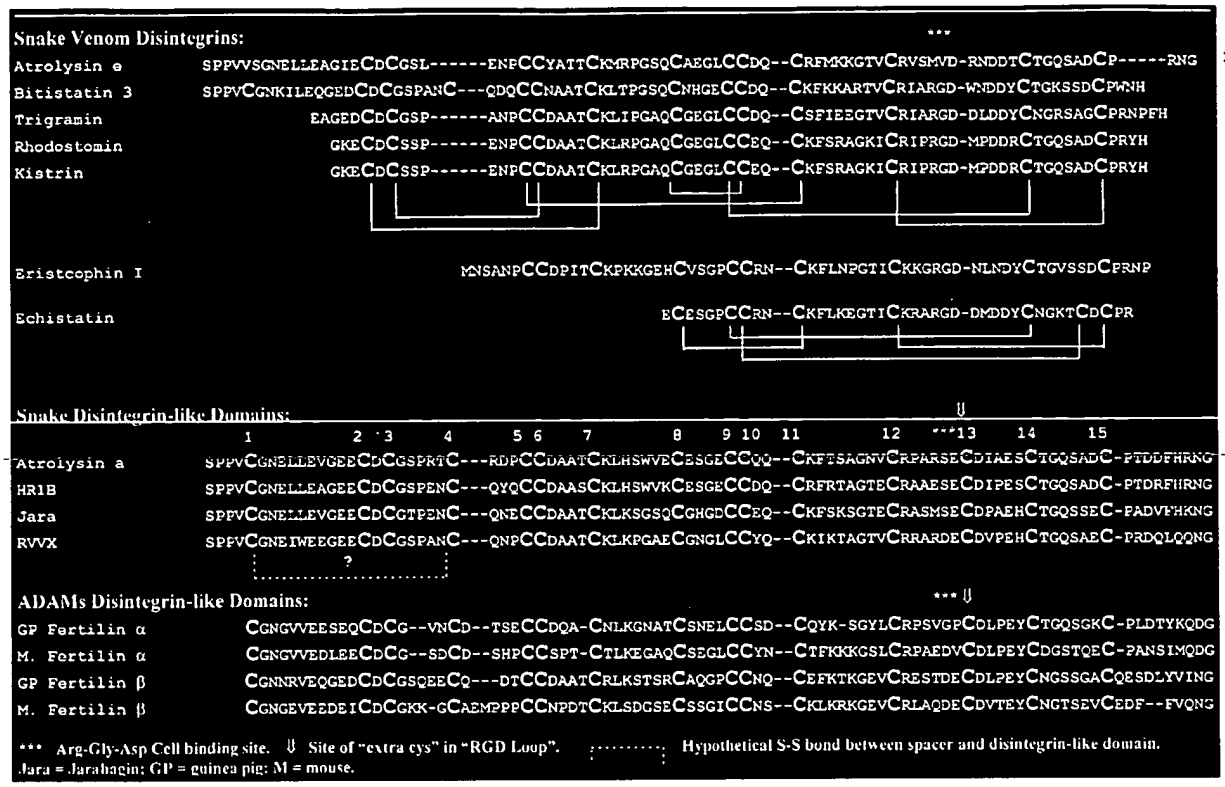

FIG. 1. **Comparison of the structure of the disintegrins with the non-RGD disintegrin-like domains of the SVMPs and the ADAMs.**

with a region amino-terminal to the disintegrin-like domain (the spacer region) which links the disintegrin-like domain with the proteinase domain (Fig. 1). The other cysteinyl residue is thought to be in a disulfide bond linkage with a cysteinyl residue in the cysteine-rich domain carboxyl to the disintegrin-like domain (22). This would form the spacer region, the disintegrin-like domain, and cysteine-rich domain into one continuous, disulfide bond-interconnected structure. The other notable difference between the disintegrin-like domains of the SVMPs and the disintegrin peptides is that while most disintegrins contain the RGD integrin-binding consensus sequence, to date no disintegrin-like domain of the class P-III SVMPs has been reported with the RGD consensus sequence. Furthermore, the additional cysteinyl residue found in the *XXCD* sequence described above for disintegrin-like domains lies in the middle of the loop where in the disintegrins the RGD sequence is located. Therefore, the topology of the disintegrin-like domain in this area is probably very different from that observed in the disintegrins proper (23, 24). This would certainly be the case if that cysteinyl residue were involved in a disulfide bond.

Since the class P-III hemorrhagic proteinases are significantly more potent than the class P-I toxins, we hypothesize that the additional carboxyl domains in the P-III toxins make an important contribution to the overall higher potency of this class of hemorrhagic toxins (22). To explore this concept, we have expressed in insect cells the combined disintegrin-like/cysteine-rich domains (A/DC) of atrolysin A, the most potent hemorrhagic toxin from the western diamondback rattlesnake *Crotalus atrox*. We now report on the ability of the recombinant A/DC protein as well as synthetic peptides designed from the SECD sequence region of the disintegrin-like domain to inhibit platelet aggregation. The structural role of the middle cysteinyl residue and adjacent acidic residues in the SECD loop region of disintegrin-like domains is also described.

EXPERIMENTAL PROCEDURES

Cloning of Atrolysin A Disintegrin-like/Cysteine-rich Domains (A/DC)—Standard recombinant DNA techniques were used to clone the A/DC fragment into the baculovirus pMbac vector (Stratagene Cloning Systems, La Jolla, CA). The DNA fragment encoding the disintegrin-like and cysteine-rich domains of atrolysin A was generated by polymerase chain reaction from an atrolysin A cDNA clone (4). Two oligonucleotide primers were designed for the polymerase chain reaction amplification and cloning. The upstream primer was 5′-CAATGACCCGGGGCAAACAGATATAATTTCAC-3′ and the downstream primer used was 5′-GATCTGGATCCTCAAATCTGAGAGAAGCCAGA-3′. These two primers were designed to include *Sma*I and *Bam*HI restriction sites, respectively, for in-frame insertion into the *SmaI/Bam*HI-linearized pMbac vector. The pMbac vector contains the signal sequence for melittin so that the recombinant protein should be secreted into the media. Prior to ligation into the pMbac vector, the A/DC polymerase chain reaction fragment (657 base pairs) was ligated into the pCR II TA cloning vector (Invitrogen) for propagation and then restriction with *SmaI/Bam*HI. The accuracy and frame information of A/DC in the pMbac vector was confirmed by complete DNA sequence and restriction analysis of the insert (25). Recombinant baculoviruses were generated by co-transfection of Sf9 (*Spodoptera frugiperda*) cells with the pMbac vector containing the A/DC insert (pMbac/A/DC) and AcNMPV nuclear polyhedrosis virus according to manufacturer's instructions (BaculoGold Transfection Kit, PharMingen). Plaque assays were performed, and following three rounds of plaque purification a population of homogeneous, recombinant A/DC baculovirus particles were obtained.

Expression and Isolation of Recombinant A/DC from Sf9 Insect Cells—Sf9 cells at a cell density of 2–3 × 10^6 cell/ml were transfected with the recombinant baculovirus at a ratio of 10 plaque-forming units per insect cell. The infected cells were harvested after 4 days by centrifugation at 4 °C for 15 min at 3000 rpm. The pelleted cells were resuspended in lysis buffer (10 mM Tris-HCl buffer, pH 8.0, 1 mM EDTA, 0.2 mM phenylmethylsulfonyl fluoride) and then disrupted in a French press. The suspension was centrifuged at 4 °C for 30 min at 15,000 × *g* and the resultant supernatant dialyzed against 20 mM Tris-HCl buffer, pH 8.0 at 4 °C. The dialyzed solution was then loaded onto a DEAE-cellulose ion-exchange column (1.5 × 40 cm) equilibrated with dialysate buffer, and the column was developed with a linear gradient of 0–1 M NaCl in the equilibration buffer. Fractions were monitored by SDS-

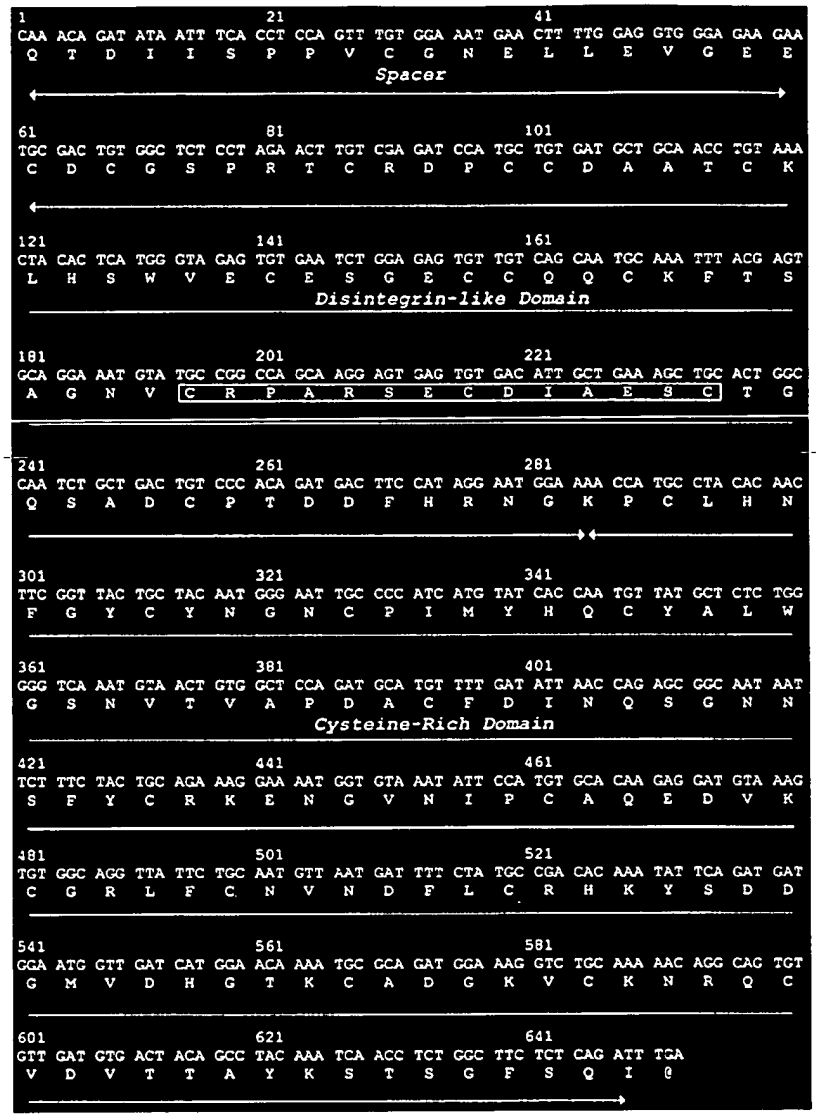

FIG. 2. **cDNA sequence and virtual protein sequence of atrolysin A/DC.** The recombinant protein sequence QTD- begins at the start spacer region. The RGD-like loop region is *boxed*.

PAGE on 12% gels (26) and by Western blot analysis using an anti-atrolysin A polyclonal antibody (27). The fractions identified as containing A/DC were pooled and dialyzed against the standard equilibration buffer. This dialyzed solution was then applied to a MonoQ 5/5 column (Pharmacia Biotech Inc.), and the column was developed with a 0–1 M NaCl gradient in the equilibration buffer. Pooled fractions containing A/DC were concentrated using a Centricon-30 concentrator (Amicon) and then loaded onto a Sephacryl S200 (Pharmacia) column (1.5 × 150 cm) developed with a 20 mM Tris-HCl buffer, pH 8.0, 100 mM NaCl, at a flow rate of 15 ml/h. Fractions containing the A/DC protein, which were homogeneous by SDS-PAGE and Western blot analysis following this chromatography, were pooled, concentrated with a Centricon-30 cartridge, and stored at −20 °C.

Characterization of Recombinant A/DC—Isolated A/DC protein was subjected to amino-terminal sequence analysis on an ABI 470A protein sequencer operated according to manufacturer's instructions. The molecular mass of A/DC was determined by MALD-TOF mass spectrometry using a Finnigan Lasermat 1000 mass spectrometer with α-cyano-4-hydroxycinnamic acid as the matrix. Atrolysin A and recombinant A/DC were alkylated under nonreducing conditions with [^{14}C]iodoacetate (53 mCi/mmol, DuPont NEN) in a 6 M guanidine HCl, 100 mM Tris-HCl, pH 7.5, alkylation buffer. Following alkylation, the proteins were desalted by reverse-phase chromatography on a C-8 (5 μm) column (5 × 30 mm) with a two-buffer gradient elution (buffer A, 0.1% trifluoroacetic acid in H_2O and buffer B, 0.1% trifluoroacetic acid in 80% $CNCH_3$ and 20% H_2O). Fractions containing ^{14}C-labeled A/DC were detected by absorbance at 214 nm, SDS-PAGE/autoradiography and by scintillation counting. Another *C. atrox* hemorrhagic metalloproteinase, atrolysin E, which has been demonstrated to contain a free cysteinyl residue (28), was subjected to the same alkylation procedure for use as a positive control.

Peptide Synthesis—All peptides were synthesized at the 50-μmol scale on a Symphony multiple peptide synthesizer (Rainin) using Fmoc (*N*-(9-fluorenyl)methoxycarbonyl) chemistry as suggested by the manufacturer and modified according to individual peptide sequences (29). Peptide amide linker resin with 0.37 mmol/g substitution (PerSeptive Biosystems) was used as the solid support. Cleavage and deprotection of the peptides were performed on the synthesizer using 88% trifluoroacetic acid, 2% diisopropylsilane, 5% H_2O, and 5% phenol. Following cleavage, the ether-extracted crude peptide product was desalted and purified on a preparative C18 reverse-phase column (250 × 21.4 mm, Rainin) using a 0.1% trifluoroacetic acid/H_2O buffer with a gradient in acetonitrile (5–80%). The purity of all peptides was assessed by analytical reverse phase-high performance liquid chromatography and MALD-TOF mass spectrometry using previously established methods (29). Only peptides deemed greater than 98% pure by reverse phase-high performance liquid chromatography were used in the platelet aggregation studies. Following synthesis, all peptides were lyophilized and stored under N_2 at −30 °C until used.

In peptide 1 (see Table I) the carboxyl-terminal cysteinyl residue was protected with an Acm group, and the cysteinyl residues at positions 1 and 8 were protected with trityl groups that were removed during cleavage of the peptide from the resin. A disulfide from Cys^1 to Cys^8 was introduced by air oxidation. Similarly, peptide 2 was synthesized by protection of cysteinyls 8 and 14 with trityl groups and cysteinyl 1 with an Acm group.

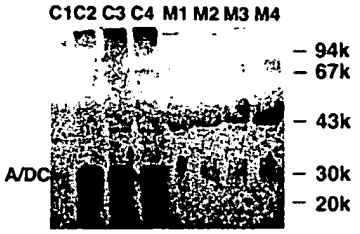

FIG. 3. **Western blot analysis of the time course of A/DC expression observed in Sf9 cells and secreted into the media.** *C1, C2, C3,* and *C4* and *M1, M2, M3,* and *M4* represent the relative amounts of A/DC found in lysed Sf9 cells and secreted into the media on days 1–4, respectively, following transfection. As can be seen, little or no specific or nonspecific background staining by anti-A/DC was observed at day 1 post-transfection (*C1*).

Peptide 3 was synthesized by protection of Cys^1 and Cys^{14} with Acm groups and Cys^8 with a trityl group. Following cleavage and deprotection, Cys^8 was alkylated with iodoacetic acid (30). Peptide 4, is based on the peptide 3 sequence except that the cysteinyl residue at position 8 is substituted by serine. Peptide 5 is based on peptide 1 structure except that the glutamyl residue at position 7 is substituted with an alanyl residue. Peptide 6 is also based on peptide 1 structure except the aspartyl residue at position 9 is substituted with an alanyl residue. Peptide 7 is the double alanyl-substituted peptide at positions 7 and 9. Peptide 8 is the Arg-Gly-Asp-Ala-substituted form of Arg-Ser-Glu-Cys sequence in peptide 3.

Platelet Aggregation Assays—Human blood was obtained from healthy donors who had not taken any medications within the previous 10 days. Blood was drawn into Becton Dickinson VACUTANER 228 containing 0.129 M sodium citrate with a final ratio of buffer to blood of 1:9. The tube was then centrifuged at 500 × *g* for 5 min. The platelet-rich plasma was transferred into a clean tube. Platelet concentration was measured with a Cell-Dyn-3000 cell counter (Abbott Diagnostics). The assay for platelet aggregation was conducted at 37 °C in an aggregometer (Payton, CO). The concentration of platelets used in each assay was 250,000 cells/μl at a final assay volume of 0.5 ml. The extent of platelet aggregation was quantitated by measuring the total amplitude at a predetermined time interval following addition of the platelet stimulant (collagen, 0.5 μg/ml, or ADP, 1 μM; ChronoLog Corp.). To assay for the ability of atrolysin A, the recombinant protein A/DC or the synthetic peptides, to inhibit platelet aggregation, the antagonists were dissolved in phosphate-buffered saline at pH 7.4, 20 mM $MgCl_2$ immediately before use. The antagonist solution was preincubated with platelet-rich plasma for 4 min at 37 °C prior to stimulation of platelet aggregation by collagen or ADP. The extent of the inhibition of platelet aggregation was assessed by comparison with the maximal aggregation induced by the control dose of agonist (1 μM ADP or 0.5 μg/ml collagen) and then expressed as a percentage. IC_{50} values were determined from dose-response curves generated from the various concentrations used for the antagonists. All experiments were performed in triplicate on blood from at least three different donors.

RESULTS

Expression, Isolation, and Characterization of Atrolysin A/DC—The translated DNA sequence for A/DC that was inserted into the pMbac vector is shown in Fig. 2. The expression of recombinant A/DC in transfected Sf9 cells was followed over time, and it was determined by Western blot analysis of Sf9 cells that day 4 post-transfected cells yielded the most product (Fig. 3). Little product was observed secreted into the medium even though a secretion expression vector had been used.

The chromatograms seen in Fig. 4 represent a typical isolation of A/DC from a 1-liter culture of Sf9 cells (2 × 10^6 cells/ml). From a 1-liter culture of transfected cells, the typical yield of purified A/DC was approximately 1 mg. The homogeneity of purified A/DC following the chromatography is seen in Fig. 5. Purified atrolysin A (4) was used as a standard for molecular weight comparison and Western blot analysis.

The amino-terminal sequence of A/DC determined from Edman degradation is given in Fig. 6. The first five residues are derived from the signal sequence of melittin, as coded for by the

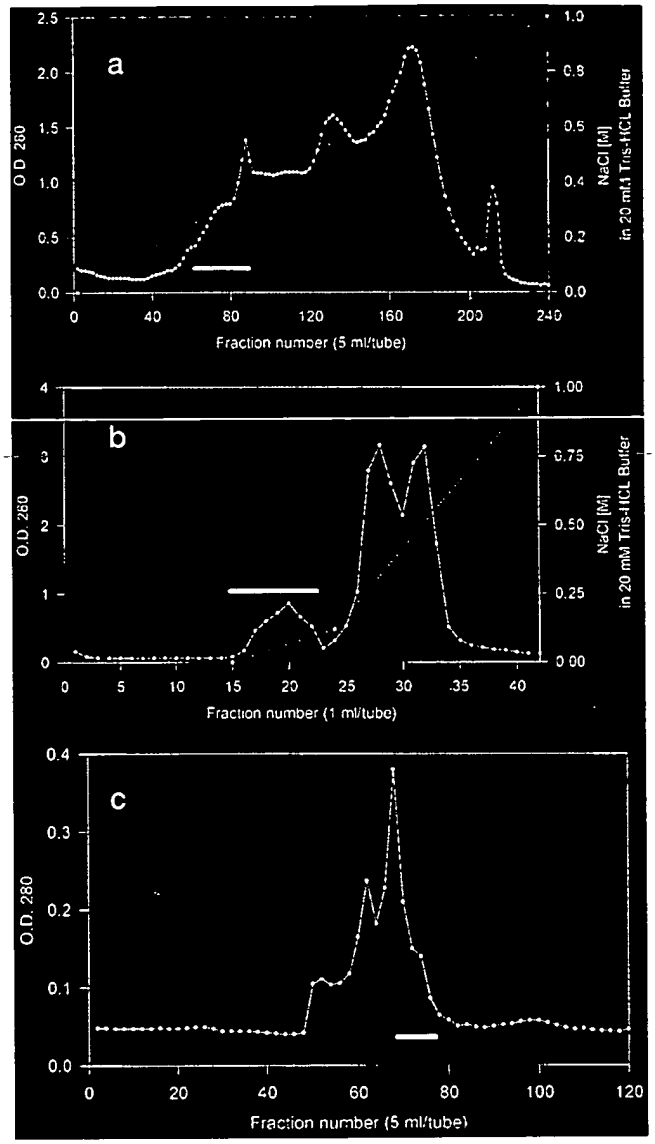

FIG. 4. **Isolation of recombinant A/DC.** *a*, DEAE-52 ion-exchange chromatography. The *dotted line* is the absorbance at 280 nm of the eluent, and the *dashed line* indicates the salt gradient. The *bar* shows the fractions where the A/DC protein was pooled. *b*, MonoQ 5/5 chromatography of the DEAE pool. The *dotted line* is the absorbance of the eluent at 280 nm, and the *dashed line* shows the elution of the salt gradient. The *bar* shows the fractions where the A/DC protein was pooled. *c*, Sephacryl S-200 gel filtration of the MonoQ pool. The *dotted line* is the absorbance of the eluent at 280 nm. The *bar* shows the fractions where A/DC was pooled.

expression vector, and are then followed by the A/DC sequence. The MALD-TOF mass spectrum of A/DC is also shown in Fig. 6. The experimental mass was determined to be 24,479 (M^+H ion) compared with 24,154 for the calculated mass, a difference of approximately 300 mass units or 1.3%. The explanation for this small discrepancy is unclear; however, there is a possibility for glycosylation of this protein. From protein sequence studies of atrolysin A, there are two *N*-linked glycosylation consensus sequences in the cysteine-rich domain, GSNVT and SGNNS (Fig. 2 and Ref. 4). Deglycosylation of A/DC with *N*-glycanase (Genzyme) caused a decrease in mass of approximately 278 mass units (data not shown) suggesting that glycosylation at one or both of those sites gives rise to the difference in the experimental *versus* the calculated mass of A/DC. The peak at 12314 mass units is the $M^{2+}H$ ion.

^{14}C-Carboxymethylation of nonreduced A/DC yielded product with no incorporation of label. Atrolysin E, which is known to have one "free" cysteine, incorporated approximately 26 mCi of ^{14}C per mmol, which relates to 0.8 cysteines/molecule of atrolysin E. This was similar to the 30 mCi of ^{14}C per mmol found in atrolysin A. The complete sequence of mature atrolysin A also has an odd number of cysteinyl residues (4). Since both atrolysin E and atrolysin A were approximately equally labeled, we concluded that atrolysin A has a single free cysteine. Furthermore, based on the lack of counts associated with the alkylation of A/DC, it was therefore concluded that all the cysteinyl residues of recombinant A/DC are involved in disulfide bonds and that the unpaired cysteinyl residue in atrolysin A resides in the metalloproteinase domain.

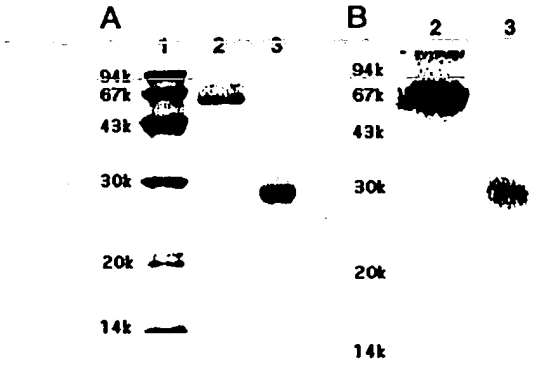

FIG. 5. **SDS-PAGE and Western blot of purified recombinant A/DC.** *A*, Coomassie Brilliant Blue-stained 12% SDS-PAGE of the pooled A/DC from the Sephacryl S-200 column. *Lane 1*, molecular mass markers; *lane 2*, atrolysin A; *lane 3*, recombinant A/DC. *B*, Western blot of identical gel. *Lane 2*, atrolysin A; *lane 3*, recombinant A/DC. Atrolysin A was purified from *C. atrox* venom according to the method of Bjarnason and Tu (45).

Platelet Aggregation Inhibition by Atrolysin A and A/DC—As seen in Figs. 7*A* and 8*A* and Table I, the hemorrhagic metalloproteinase atrolysin A was a potent inhibitor of collagen and ADP-stimulated platelet aggregation. The recombinant A/DC protein was also a potent inhibitor of platelet aggregation (Figs. 7*B* and 8*B* and Table I) but not to the same extent as atrolysin A, having a 4.3-fold greater IC_{50} value than atrolysin A for collagen-stimulated platelets. The IC_{50} of A/DC was of the same order of magnitude as observed for the disintegrins. Reduction and carboxyamidomethylation of A/DC caused a loss of all inhibitory activity (data not shown).

Platelet Aggregation Inhibition by Synthetic Peptides—The IC_{50} values for inhibition of collagen-stimulated platelet aggregation by synthetic peptides are seen in Table I. Peptide **1**, which is the cyclized Cys^1-Cys^8 disintegrin-like region was a potent inhibitor of collagen-stimulated platelet aggregation with an IC_{50} of 218 ± 42 μM (Fig. 9). Peptide **2**, which was the Cys^8-Cys^{14} form of the peptide, also was demonstrated to be an inhibitor of platelet aggregation with an IC_{50} of 391 ± 31 μM. Peptide **3** which is a linear peptide where the Cys^8 is alkylated and hence not constrained in a disulfide bond lacks inhibitory activity. Similarly, peptide **4**, in which the Cys^8 of peptide **3** is substituted by a serinyl residue, also lacks activity. Peptides **5**, **6**, and **7** represent an alanine scanning substitution for the Glu^7 and Asp^9 residues adjacent to Cys^8. In peptide **5**, which has a Glu^7 → Ala substitution, there is an approximate 2.5 decrease in activity compared with peptide **1**. Peptide **6**, which has an Asp^9 → Ala substitution, the IC_{50} value is approximately 1000 μM. When both the Glu^7 and Asp^9 are substituted with alanyl residues there is an even greater decrease in activity, with an apparent IC_{50} value significantly greater than 1 mM; however, due to peptide solubility, a more precise value

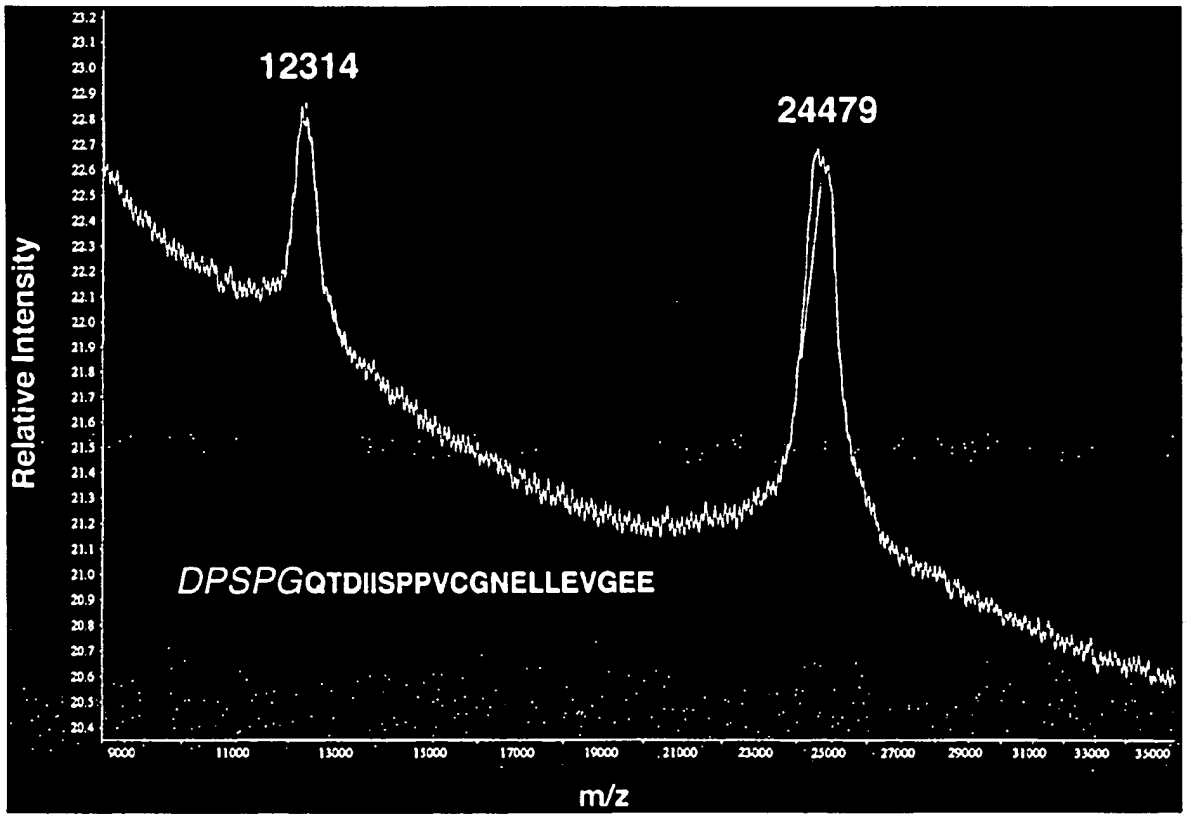

FIG. 6. **MALD-TOF mass spectrum of recombinant A/DC.** The amino terminus of recombinant A/DC as determined by Edman degradation is shown in the *inset*. The first five amino acids (*in italic*) are part of the melittin signal peptide.

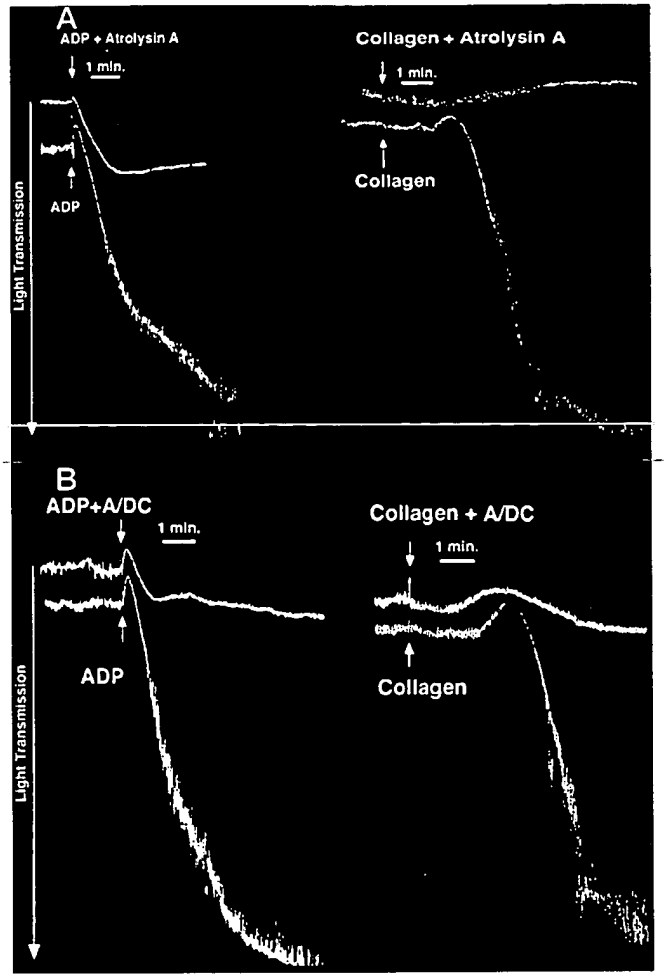

FIG. 7. **Effect of atrolysin A on human platelet aggregation.** *A*, aggregometer tracings of ADP-induced (2 μM) and collagen I-induced (0.5 μg/ml) human platelet aggregation inhibited by atrolysin A (0.3 μM). *B*, aggregometer tracing of ADP-induced (2 μM) and collagen I-induced (0.5 μg/ml) human platelet aggregation inhibited by A/DC (1.0 μM).

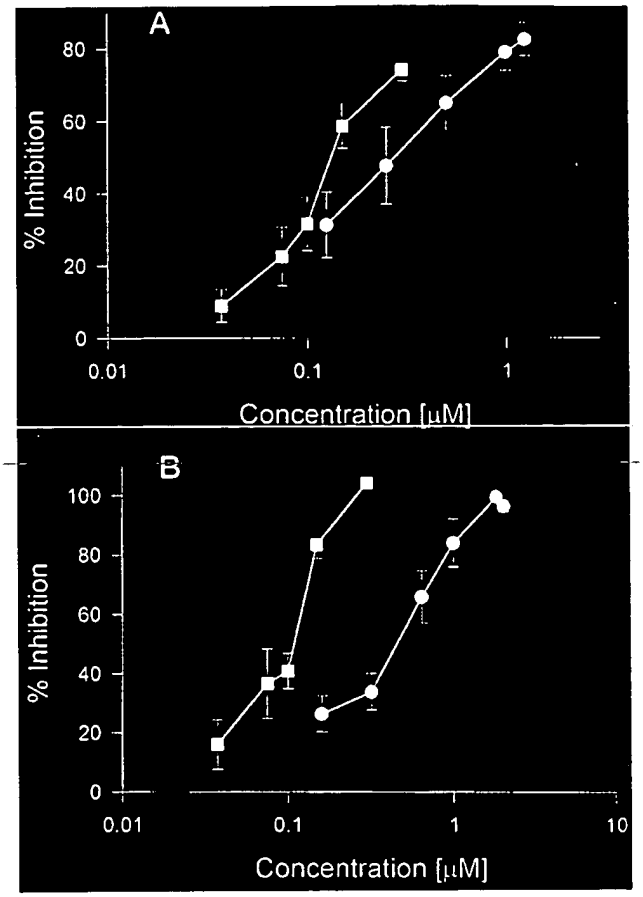

FIG. 8. **Concentration dependence of atrolysin A and A/DC inhibition of ADP-induced (2 μM) (*A*) or collagen I-induced (0.5 μg/ml) (*B*) human platelet aggregation.** Each *curve* represents the mean of 3–6 individual experiments. The *squares* represent the atrolysin A data and the *circles* A/DC.

could not be obtained. Peptide 8, which is the RGDA-substituted form of the RSEC residues in peptide 1, was demonstrated to have potent collagen and ADP-stimulated platelet aggregation inhibition activity. The IC_{50} values for both collagen and ADP-stimulated platelet aggregation inhibition by peptide 1 are of the same order of magnitude for those observed with linear RGD containing peptides (14).

The protein inhibitors of platelet aggregation, such as atrolysin A, the recombinant A/DC protein, and the disintegrins themselves are significantly more active than their RGD/RGD-like loop peptide derivatives. Therefore, upon consideration of these data, it may be concluded that additional structural features other than those represented simply by a linear array of amino acids in the synthetic peptides, even though they are somewhat structurally constrained, are essential for the full inhibitory potential of these proteins.

DISCUSSION

It is generally observed that the higher molecular weight hemorrhagic metalloproteinases from snake venoms, as represented by the class P-III toxins, are significantly more toxic than the P-I class toxins (1). For example, the minimum hemorrhagic dose of atrolysin E, the most potent class P-II hemorrhagic toxin from the western diamondback rattlesnake *C. atrox*, is 1 μg/mouse. Atrolysin A, also from *C. atrox* venom, is a P-III toxin, which in addition to its proteinase domain has disintegrin-like and cysteine-rich domains. Its minimum hemorrhagic dose is 0.04 μg, making atrolysin A 25 times more hemorrhagic than atrolysin E, which in its mature form contains only a metalloproteinase domain. This observation led to our hypothesis that the additional domains of the P-III toxins contribute to their greater hemorrhagic potency. The functionality explored in this study is whether the disintegrin-like domain of the P-III toxins can serve to inhibit platelet aggregation and thus potentiate the production of hemorrhage.

The ability of atrolysin A to inhibit platelet aggregation is an interesting and novel observation stemming from this study. Unfortunately, due to the presence of three domains in atrolysin A, each with its own potential biological activity, it is unclear which domain(s) is responsible for the inhibition of platelet aggregation. The investigation into the contribution of the disintegrin-like domain of atrolysin A to inhibit platelet aggregation required expression of that recombinant domain. Expression of the disintegrin-like domain of atrolysin A failed to produce monomer product; therefore, we constructed and expressed in insect cells a recombinant protein comprised of the spacer region/disintegrin-lik and the cysteine-rich domains of atrolysin A. The failure to express the disintegrin-like domain alone may be attributed to the possibility that there is one disulfide bond linking the spacer region with the disintegrin-like domain and one disulfide bond linking the disintegrin-like domain with a cysteinyl residue in the cysteine-rich domain (Fig. 2 and Ref. 22). This hypothesis is based on the

TABLE I

Inhibition of platelet aggregation by recombinant A/DC and synthetic peptides

NI, no inhibition; Acm, acetoamidomethylated cysteine; Ac, acetylated amino terminus; ND, not determined. Number in parentheses is the number of different donors used to generate data. S.E., standard error of the mean.

	Inhibitor	Platelet stimulant	
		Collagen (0.5 μg/ml)	ADP (1 μM)
		IC_{50} [μM] ± S.E.	
Atrolysin A		0.11 ± 0.01 (4)	0.24 ± 0.16 (3)
Recombinant A/DC		0.47 ± 0.05 (6)	0.32 ± 0.06 (4)
Peptide			
1	Ac-CRPARSECDIAESC(Acm)-NH_2	218 ± 42 (6)	ND
2	Ac-C(Acm)RPARSECDIAESC-NH_2	391 ± 31 (3)	ND
3	Ac-C(Acm)RPARSEC(cm)DIAESC(Acm)-NH_2	NI	NI
4	Ac-C(Acm)RPARSESDIAESC(Acm)-NH_2	NI	NI
5	Ac-CRPARSACDIAESC(Acm)-NH_2	546 ± 146 (3)	ND
6	Ac-CRPARSECAIAESC(Acm)-NH_2	~1000 (3)	ND
7	Ac-CRPARSACAIAESC(Acm)-NH_2	>>1000 (3)	ND
8	Ac-C(Acm)RPARGDADIAESC(Acm)-NH_2	156 ± 34 (3)	65 ± 3 (3)

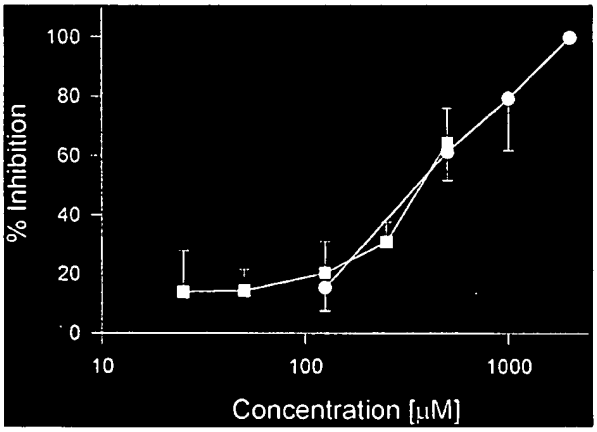

FIG. 9. **Concentration dependence of cyclized synthetic RGD-like loop peptides on collagen I (0.5 μg/ml)-induced human platelet aggregation.** *Circles* represent peptide 1, CRPARSECDIAESC(Acm) and *squares* represent peptide 2, (Acm)CRPARSECDIAESC.

comparison of the structures of disintegrin-like domains of the SMVPs and the ADAMs groups of the reprolysins to the structures of various venom disintegrins (4, 8, 14, 22, 31, 32). Ultimately, determination of the disulfide bond arrangement in the disintegrin-like and cysteine-rich domains of the P-III class of snake venom metalloproteinases will be necessary to prove the hypothesis.

Baculovirus expression of recombinant A/DC in insect cells was successful, ultimately yielding a protein with the ability to inhibit both collagen- and ADP-stimulated platelet aggregation. This suggests that A/DC is acting at the level of the $\alpha_2\beta_1$ collagen integrin and/or the fibrinogen receptor, $\alpha_{IIb}\beta_3$, on platelets (33–35). From the studies with the synthetic peptides one may conclude that the functional portion of A/DC involved in platelet binding resides in the disintegrin-like domain. However, at this point we have no direct evidence to exclude interactions with platelet integrins through the cysteine-rich domain of A/DC. The hemorrhagic toxin jararhagin, which is a structural homologue of atrolysin A, has been demonstrated to bind to the α_2 subunit of the $\alpha_2\beta_1$ integrin to inhibit platelet adhesion to collagen (36). Jararhagin has also been shown to cause the proteolytic loss of the platelet collagen receptor, $\alpha_2\beta_1$, and to degrade the adhesive plasma protein von Willebrand factor (37).

Although A/DC blocked platelet aggregation, it was somewhat less potent than atrolysin A. Whether this reflects the presence of additional inhibitory motifs in the structure of atrolysin A or the proteolytic effects of the metalloproteinase domain of atrolysin A, as appears to be the case with jararhagin, is unknown. Alternatively, the recombinant structure may not reflect the actual structure of the disintegrin-like domain as found in the P-III toxins. IC_{50} values for ADP-stimulated platelet aggregation inhibition by snake venom disintegrins range from approximately 100 to 555 nM (14, 16). The IC_{50} values of atrolysin A and recombinant A/DC for ADP-stimulated platelet aggregation inhibition determined in this study were 240 and 320 nM, respectively, which are comparable to those observed for the disintegrins. This similarity of potency of A/DC to the disintegrins is of great interest given the significant differences in the sequences in this region of the disintegrin (-like) domains of these proteins, particularly in the sense that A/DC lacks the cell-binding RGD consensus sequence. However, it has been reported that the RGD sequence need not be strictly conserved in the disintegrins for a potent ability to inhibit platelet aggregation (38, 39). In the case of barbourin, the disintegrin isolated from *Sistrurus miliarus barbouri*, in lieu of the RGD sequence, there is a conserved substitution of the arginine with lysine (39). This disintegrin has an IC_{50} value for inhibition of platelet aggregation similar to that observed for RGD-containing disintegrins (14). In another example, using a murine Fab fragment specific for the integrin $\alpha_{IIb}\beta_3$, Kunicki and colleagues (40) demonstrated that the cognate RGD sequence could be exchanged with RYD without an alteration in integrin recognition. These data suggest that some limited diversity in this sequence region may be tolerated and still give rise to a ligand with reasonable potency for inhibiting aggregation.

From structural studies of several disintegrins, the RGD sequence is found positioned within an extended, flexible β-loop structure where there is only limited conformational restriction of the RGD sequence (24, 32, 41, 42). Unfortunately, no similar structural information is available for disintegrin-like domain containing proteins. Reduction and alkylation of disintegrins cause a significant loss of platelet aggregation inhibition activity (19, 20), which is also the case with A/DC. Therefore, as in the disintegrins, the constrained display in this region in the disintegrin-like domain of A/DC is critical for activity. Never-

theless, there remain structural differences between these regions of the disintegrin-like domain and the disintegrins based on their differences in sequence, disulfide bonding patterns, and biological activities.

Using synthetic peptides, we have shown that the SECD sequence region in the disintegrin-like domain of A/DC is involved in platelet aggregation inhibitory activity. This region is the positional homologue of the RGD loop of the disintegrins. The two significant differences between this region of the disintegrin-like domains of the SVMPs and the RGD region of the disintegrins are the *XX*(E/*D*)CD substitution for RGD*XX* sequences observed in the disintegrins and the presence of a disulfide bonded cysteinyl residue (SECD) in the disintegrin-like domain region. Given these significant differences, it is very interesting that A/DC should have any ability to inhibit platelet aggregation and suggests a somewhat different interaction of this region of the disintegrin-like domain with the platelet $\alpha_{IIb}\beta_3$ integrin compared with that for the RGD disintegrins.

We have shown that the RSECD cysteinyl residue in atrolysin A and the recombinant A/DC is constrained by a disulfide bond. Although the synthetic peptides we tested were disulfide bonded from Cys^1 to Cys^8 or Cys^8 to Cys^{14}, this does not suggest that it is the same bonding pattern that occurs in the protein. However, since the RSECD cysteinyl residue is disulfide bonded in atrolysin A and A/DC, that region must be conformationally constrained with a quite different topology compared with the 13-member RGD loop of the disintegrins. This structural difference of the *XX*CD region of the disintegrin-like domain appears to be crucial for activity since the synthetic, linear peptides, which lack disulfide bonds or a free sulfhydryl, did not inhibit platelet aggregation.

A protein containing a disintegrin-like domain, which lacks a metalloproteinase domain, has been isolated and characterized from *Bothrops jararaca* venom and has a similar structure to the recombinant A/DC protein constructed for this study. This protein, jararhagin-C, begins with an amino-terminal sequence homologous to the spacer region of the P-III toxins followed by disintegrin-like and cysteine-rich sequences (43). Jararhagin-C can inhibit ADP- and collagen-induced platelet aggregation. The sequence of jararhagin-C is identical to the spacer/disintegrin-like/cysteine-rich domains of jararhagin, a 55-kDa hemorrhagic toxin from *B. jararaca* (44). Therefore, jararhagin-C is a proteolytically processed form of jararhagin. In this study, we have demonstrated that atrolysin A and the recombinant protein A/DC, comprised of the spacer/disintegrin-like/cysteine-rich domains, have potent platelet aggregation inhibitory activities. These data suggest an increased complexity for the venom of crotalid snakes from the standpoint of hemorrhagic toxicity. The high molecular weight P-III toxins can cause hemorrhage by direct proteolytic disruption of capillary basement membranes (31). They may also synergize hemorrhage production by inhibiting platelet aggregation via their disintegrin-like domain and by proteolysis of integrins and plasma adhesive proteins with their metalloproteinase domain. Indeed, the disintegrin-like and cysteine-rich domains may participate in the proteolytic specificity of these P-III toxins by directing them to the appropriate substrates. Hemorrhagic toxins are present in crotalid venoms, and their proteolytically processed fragments are comprised of spacer/disintegrin-like/cysteine-rich domains, as well as the disintegrins proper, all of which give rise to a very potent mixture of active proteins contributing to hemorrhage production and inhibition of platelet aggregation. Therefore, it is understandable that hemorrhage production is one of the foremost pathological consequences of crotalid snake envenomation.

In summary we have shown that the class P-III hemorrhagic toxin, atrolysin A from *C. atrox*, is a potent inhibitor of platelet aggregation. Our studies with synthetic peptides demonstrate that the region of the disintegrin-like domain of atrolysin A which is positionally analogous to the RGD loop of the disintegrins is primarily responsible for blocking platelet aggregation. The RSECD sequence in the disintegrin-like domain requires conformational restriction through disulfide bonding of the cysteinyl residue for biological activity. These considerations, plus the fact that the critical sequence is not an RGD sequence, suggest that different structural parameters are responsible for the biological activity of the disintegrin-like domains of the P-III toxins and the disintegrin-like domains of the ADAMs/MDC proteins. The data reported in this study provide a new structural framework for the development of novel integrin antagonists.

Acknowledgments—We thank Dr. John Humphries and John Sanders, University of Virginia Health Sciences Center, for their assistance with the platelet aggregation studies and Dr. Adrian Gear, University of Virginia Health Sciences Center, for the scientific discussions of the data and critical reading of the manuscript.

REFERENCES

1. Bjarnason, J. B., and Fox, J. W. (1995) *Methods Enzymol.* **248**, 345–367
2. Teng, C.-M., and Huang, T.-F. (1991) *Platelets* **2**, 1–11
3. Bjarnason, J. B., and Fox, J. W. (1994) *J. Pharmacol. Exp. Ther.* **62**, 321–372
4. Hite, L. A., Jia, L.-G., Bjarnason, J. B., and Fox, J. W. (1994) *Arch. Biochem. Biophys.* **308**, 182–191
5. Rawlings, N. D., and Barrett, A. J. (1995) *Methods Enzymol.* **248**, 183–228
6. Primakoff, P., Hyatt, H., and Tredick-Kline, J. (1987) *J. Cell Biol.* **104**, 141–149
7. Wolfsberg, T. G., Bazan, J. F., Blobel, C. P., Myles, D. G., Primakoff, P., and White, J. M. (1993) *Proc. Natl. Acad. Sci. U. S. A.* **90**, 10783–10787
8. Wolfsberg, T. G., Straight, P. D., Gerena, R. L., Huovila, A.-P. J., Primakoff, P., Myles, D. G., and White, J. M. (1995) *Dev. Biol.* **169**, 378–383
9. Perry, A. C. F., Barker, H. L., Jones, R., and Hall, L. (1994) *Biochim. Biophys. Acta* **1207**, 134–137
10. Almeida, E. A. C., Huovila, A.-P. J., Sutherland, A. E., Stephens, L. E., Calarco, P. G., Shaw, L. M., Mercurio, A., M., Sonnenberg, A., Primakoff, P., Myles, D. G., and White, J. M. (1995) *Cell* **81**, 1095–1104
11. Yagami-Hiromasa, T., Sato, T., Kurisaki, T., Kamijo, K., Nabeshima, Y.-I., and Fujisawa-Sehara, A. (1995) *Nature* **377**, 652–656
12. Rooke, J., Pan, D., Xu, T., and Rubin, G. M. (1996) *Science* **273**, 1227–1230
13. Myles, D. G., Kimmel, L. H., Blobel, C. P., White, J. M., and Primakoff, P. (1994) *Proc. Natl. Acad. Sci. U. S. A.* **91**, 4195–4198
14. Niewiarowski, S., McLane, M. A., Kloczewiak, M., and Stewart, G. J. (1994) *Semin. Hematol.* **31**, 289–300
15. Gould, R. J., Polokoff, M. A., Friedman, P. A., Huang, T. F., Holt, J. C., Cook, J. J., and Niewiarowski, S. (1990) *Proc. Soc. Exp. Biol. Med.* **195**, 168–171
16. Dennis, M. S., Henzel, W. J., Pitti, R. M., Lipari, M. T., Napier, M. A., Deisher, T. A., Bunting, S., and Lazarus, R. A. (1989) *Proc. Natl. Acad. Sci. U. S. A.* **87**, 2471–2475
17. Dennis, M. S., Carter, P., and Lazarus, R. A. (1993) *Proteins* **15**, 312–321
18. Lazarus, R. A., and McDowell, R. S. (1993) *Curr. Opin. Biotechnol.* **4**, 438–443
19. Calvete, J. J., Schäfer, W., and Soszka, T. (1991) *Biochemistry* **30**, 5225–5229
20. Gan, Z.-R., Gould, R. J., Jacobs, J. W., Friedman, P. A., and Polokoff, M. A. (1988) *J. Biol. Chem.* **263**, 19827–19832
21. Au, L.-C., Chou, J.-S., Chang, K.-J., Teh, G. W., and Lin, S. B. (1993) *Biochim. Biophys. Acta* **1173**, 243–245
22. Fox, J. W., and Bjarnason, J. B. (1996) in *Zinc Metalloproteinases in Health and Disease* (Hooper, N. M., ed) pp. 47–82, Taylor & Francis Ltd., London
23. Gray, W. R. (1993) *Protein Sci.* **2**, 1749–1755
24. Adler, M., Carter, P., Lazarus, R. A., and Wagner, G. (1993) *Biochemistry* **32**, 282–289
25. Sanger, F., Nicklen, S., and Coulson, A. R. (1977) *Proc. Natl. Acad. Sci. U. S. A.* **74**, 5463–5467
26. Laemmli, U. K. (1979) *Nature* **227**, 680–685
27. Burnette, W. N. (1981) *Anal. Biochem.* **112**, 195–203
28. Hite, L. A., Shannon, J. D., Bjarnason, J. B., and Fox, J. W. (1992) *Biochemistry* **31**, 6203–6211
29. Pöschl, E., Fox, J. W., Block, D., Mayer, U., and Timpl, R. (1994) *EMBO J.* **13**, 3741–3747
30. Crestfield, A. M., Moore, S., and Stein, W. H. (1963) *J. Biol. Chem.* **238**, 622–627
31. Baramova, E. N., Shannon, J. D., Bjarnason, J. B., and Fox, J. W. (1989) *Arch. Biochem. Biophys.* **275**, 63–71
32. Atkinson, R. A., Saudek, V., and Pelton, J. T. (1994) *Int. J. Pept. Protein Res.* **43**, 563–572
33. Phillips, D. R., Charo, I. F., and Scarborough, R. M. (1991) *Cell* **65**, 359–362
34. McLane, M. A., Kowalska, M. A., Silver, L., Shattil, S. J., and Niewiarowski, S. (1994) *Biochem. J.* **301**, 429–436
35. Ginsberg, M. H., Du, X., O'Toole, T. E., and Loftus, J. C. (1995) *Thromb. Haemostasis* **74**, 352–359
36. De Luca, M., Ward, C. M., Ohmori, K., Andrews, R. K., and Berndt, M. C. (1995) *Biochem. Biophys. Res. Commun.* **206**, 570–576

37. Kamiguti, A. S., Hay, C. R. M., Theakston, R. D. G., and Zuzel, M. (1996) *Toxicon* **34**, 627–642
38. Scarborough, R. M., Rose, J. W., Hsu, M. A., Phillips, D. R., Fried, V. A., Campbell, A. M., Nannizzi, L., and Charo, I. F. (1991) *J. Biol. Chem.* **266**, 9359–9362
39. Scarborough, R. M., Rose, J. W., Naughton, M. A., Phillips, D. R., Nannizzi, L., Arfsten, A., Campbell, A. M., and Charo, I. F. (1993) *J. Biol. Chem.* **268**, 1058–1065
40. Kunicki, T. J., Ely, K. R., Kunicki, T. C., Yomiyama, Y., and Annis, D. S. (1995) *J. Biol. Chem.* **270**, 16660–16665
41. Aumailley, M., Gurrath, M., Müller, G., Calvete, J., Timpl, R., and Kessler, H. (1991) *FEBS Lett.* **291**, 50–54
42. Gurrath, M., Müller, G. Kessler, H., Aumailley, M., and Timpl, R. (1992) *Eur. J. Biochem.* **210**, 911–921
43. Usami, Y., Fuimura, Y., Miura, S., Shima, H., Yoshida, E., Yoshioka, A., Hirano, K., Suzuki, M., and Titani, K. (1994) *Biochem. Biophys. Res. Commun.* **201**, 331–339
44. Paine, M. J. I., Desmond, H. P., Theakston, R. D. G., and Crampton, J. M. (1992) *J. Biol. Chem.* **267**, 22869–22876
45. Bjarnason, J. B., and Tu, A. T. (1978) *Biochemistry* **17**, 3395–3404